ARCHIVES OF ACOUSTICS
29, 4, 577–596 (2004)

GA OPTIMIZATION ON SINGLE-CHAMBER MUFFLER HYBRIDIZED WITH EXTENDED TUBE UNDER SPACE CONSTRAINTS

Y.-C. CHANG, L.-J. YEH, M.-C. CHIU

Tatung University
Department of Mechanical Engineering
Taipei, Taiwan 104, R.O.C.
email: min-chie.chiu@etci.com.tw,
ljyeh@ttu.edu.tv, cchang@ttu.edu.tw

(*received 27 November 2003; accepted 23 September 2004*)

Mufflers are habitually adopted in gas venting systems under space constraint for maintenance and operation. The shape optimization in the muffler to maximize the sound performance is then highly focused, accordingly.

In this paper, the shape design of a muffler with extended tubes optimized by the genetic algorithm (GA) is presented. A numerical case in eliminating the pure tone noise is introduced. Before optimization, the mathematical model is compared by the experimental data for an accuracy check. The results indicate that the sound transmission loss (STL) is maximized exactly at the designed frequency. Consequently, we demonstrate a successful GA application on the muffler design.

Key words: single-chamber muffler hybridized with extended tube, transfer matrix method, space constraints, GA optimization.

Notations

This paper is constructed on the basis of the following notations:

bit_n	bit length,
C_0	sound speed ($\mathrm{m\,s^{-1}}$),
C_v	specific heat at constant volume ($\mathrm{kJ\ kg^{-1}\ ^\circ K}$),
D	diameter (m),
elt_no	selection of elite (1 for yes and 0 for no),
gen_no	maximum no. of generation,
f	cyclic frequency (Hz),
j	$\sqrt{-1}$,
k	wave number (w/c_o),
K_c	stagnation pressure loss factor between point 5 and point 7,
K_e	stagnation pressure loss factor between point 2 and point 4,

L_i length of the i-th segment of silencer (m),
M_i mean flow Mach number at i,
pc: crossover ratio,
$p_{c,i}$ aeroacoustic pressure at i (Pa),
p_i pressure; acoustic pressure at i (Pa),
pm: mutation ratio,
popuSize: no. of population,
p_o pressure of steady flow (Pa),
Q volume flow rate of venting gas (m^3/s),
R gas constant,
$rt1$ length ratio ($= L_2/L_3$),
$rt2$ length ratio ($= L_4/L_3$),
u_i acoustic particle velocity at i (m s^{-1}),
V_i mean flow velocity at i (m s^{-1}),
$\nu_{c,i}$ aeroacoustic mass velocity at i (kg s^{-1}),
S_i section area at i (m^2),
STL sound transmission loss (dB),
Y_i characteristic impedance at i ($Y_i = c_o/S_i$),
ρ_i fluctuated density at i (kg m^{-3}),
ρ_o air density of steady flow (kg m^{-3}),
γ specific heat ratio of air.

1. Introduction

Nowadays, the low noise level of a product has become an essential factor in sales and profit [1]. Nevertheless, the shape of muffler is often confined in the limited space volume for obligation of operation and maintenance. Besides, the discussion of optimal design under space constraints is rarely emphasized even if many researches of muffler design have been well addressed. BERNHARD [2] has introduced the shape optimization of simple expansion mufflers by using design sensitivity matrices. The space volume of the reactive silencer is still non-constrained, and the calculation of the design sensitivity matrices is complicated. In the previous work [3], the graphical analysis of optimal shape design to improve the performance of STL on a constrained single expansion muffler was discussed. Thus, to enhance the STL on the muffler, a new constrained muffler hybridized with an extended tube is introduced.

In addition, either of the traditional gradient methods or random searching techniques is not easy to use in shape optimization of the muffler design with an extended tube, conjugated with the space constrain problem and highly nonlinear in the objective function. The former one lacks of the ability of searching candidate solutions in the wide band of database and often falls into the local optimum. The latter one spends a large of time in a random search over the whole database which is very inefficiently. To overcome these weakness occurred in the classical methods, a genetic algorithm (GA) [4] based on the evolution theorem of Darwin principles is therefore introduced for the implementation of optimization of the muffler design problem in this paper. In this paper, GA is coupled with the transfer matrix method [5, 6], which is the basis of the plane wave theory and is easier in evaluating the STL of the muffler.

2. Theoretical background

In this paper, the single-chamber muffler with extended tube is discussed. For the ease of the theoretical derivation on muffler, two kinds of muffler components, including (1) a straight duct and (2) a extended duct, are firstly identified and depicted in Fig. 1. On the basis of plane wave theorem, the derivations of the four-pole transfer matrix is deduced by neglecting the higher-order waves generated due to the effects of nonlinear dissipation, high speed flowing and rotation. With the deduced transfer matrices and the combination, the complete four-pole matrix of the whole muffler can be built. Furthermore, the STL can be easily calculated by means of the four-pole matrix. By the classification of the distinct component in muffler, three elements of the straight ducts and two elements of the extended ones are distinguished. The muffler's flowing condition and location is specified in Fig. 2, where the whole flow condition within the muffler can be represented by eight nodes (pt1$\sim$pt8) of acoustic pressure – p_i and the acoustic particle velocity – u_i that are chosen within each elements individually. The theoretical derivation for each element is illustrated as follows.

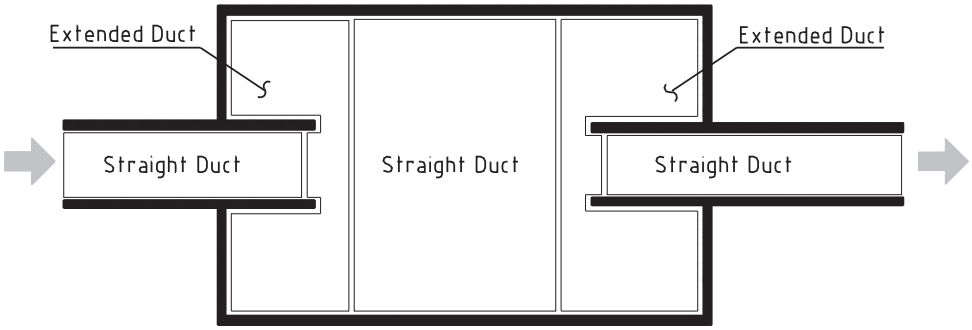

Fig. 1. Distinction of the muffler elements.

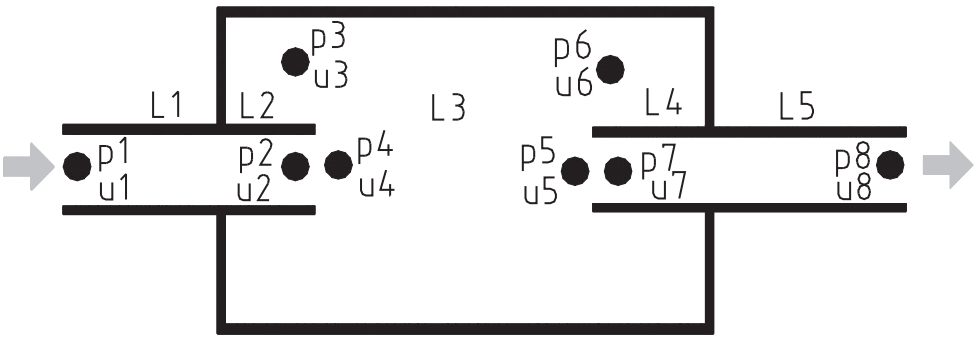

Fig. 2. Flow conditions for a single-chamber muffler with extended tubes.

2.1. *Straight duct* [5]

As derived by PRASAD [5], the four-pole matrix between point 1 and point 2 with mean flow is expressed in Eq. (1)

$$\begin{pmatrix} p_1 \\ \rho_o c_o u_1 \end{pmatrix} = e^{-jM_1 k(L_1+L_2)/(1-M_1^2)} \begin{bmatrix} b11^* & b12^* \\ b21^* & b22^* \end{bmatrix} \begin{pmatrix} p_2 \\ \rho_o c_o u_2 \end{pmatrix}, \tag{1}_1$$

where

$$\begin{aligned} b11^* &= \cos\left[\frac{k(L_1+L_2)}{1-M_1^2}\right], \qquad b21^* = j\sin\left[\frac{k(L_1+L_2)}{1-M_1^2}\right], \\ b12^* &= j\sin\left[\frac{k(L_1+L_2)}{1-M_1^2}\right], \qquad b22^* = \cos\left[\frac{k(L_1+L_2)}{1-M_1^2}\right]. \end{aligned} \tag{1}_2$$

As the derivation in Eq. (1), the four-pole matrix between point 4 and point 5 with mean flow is expressed in Eq. (2).

$$\begin{pmatrix} p_4 \\ \rho_o c_o u_4 \end{pmatrix} = e^{-jM_5 kL_3/(1-M_5^2)} \begin{bmatrix} c11^* & c12^* \\ c21^* & c22^* \end{bmatrix} \begin{pmatrix} p_5 \\ \rho_o c_o u_5 \end{pmatrix}, \tag{2}_1$$

where

$$\begin{aligned} c11^* &= \cos\left(\frac{kL_3}{1-M_5^2}\right), \qquad c21^* = j\sin\left(\frac{kL_3}{1-M_5^2}\right), \\ c12^* &= j\sin\left(\frac{kL_3}{1-M_5^2}\right), \qquad c22^* = \cos\left(\frac{kL_3}{1-M_5^2}\right). \end{aligned} \tag{2}_2$$

Thus, the four-pole matrix between point 7 and point 8 with mean flow is expressed in Eq. (3).

$$\begin{pmatrix} p_7 \\ \rho_o c_o u_7 \end{pmatrix} = e^{-jM_7 k(L_4+L_5)(1-M_7^2)} \begin{bmatrix} d11^* & d12^* \\ d21^* & d22^* \end{bmatrix} \begin{pmatrix} p_8 \\ \rho_o c_o u_8 \end{pmatrix}, \tag{3}_1$$

where

$$\begin{aligned} d11^* &= \cos\left[\frac{k(L_4+L_5)}{1-M_7^2}\right], \qquad d21^* = j\sin\left[\frac{k(L_4+L_5)}{1-M_7^2}\right], \\ d12^* &= j\sin\left[\frac{k(L_4+L_5)}{1-M_7^2}\right], \qquad d22^* = \cos\left[\frac{k(L_4+L_5)}{1-M_7^2}\right]. \end{aligned} \tag{3}_2$$

2.2. *Extended duct* [6, 7]

For the steady flow with aeroacoustical perturbation, the equation of mass continuity between point 5 and point 7 with mean flow is

$$(\rho_o + \rho_5)S_5(V_5 + u_5) = (\rho_o + \rho_7)S_7(V_7 + u_7) + \rho_o S_6 u_6. \tag{4}$$

As derived by MUNJAL [6], after substitution of thermodynamic properties and the neglect of the second-order terms, this yields

$$c_o\rho_o S_5 u_5 + S_5 M_5 p_5 = c_o\rho_o S_7 u_7 + c_o\rho_o S_6 u_6 + S_7 M_7 \left(p_7 - \frac{p_o}{C_v} \frac{RK_c M_7 Y_7}{p_o} \frac{v_{c,7} - M_7 p_{c,7}/Y_7}{1 - M_7^2} \right), \tag{5}_1$$

or

$$c_o\rho_o S_5 u_5 + S_5 M_5 p_5 = c_o\rho_o S_7 u_7 + c_o\rho_o S_6 u_6 + S_7 M_7 \left(p_7 - \frac{p_o(\gamma-1) K_c M_7 Y_7}{p_o} \frac{v_{c,7} - M_7 p_{c,7}/Y_7}{1 - M_7^2} \right), \tag{5}_2$$

where

$$K_c = \frac{1 - S_7/S_5}{2}. \tag{5}_3$$

For the area discontinuity across which the flow is adiabatic but not isentropic, a drop in the stagnation pressure and an increment of entropy will occur.

The concept of static enthalpy deduced by MUNJAL [5, 6] is described as

$$\begin{bmatrix} p_{c,7} \\ \\ v_{c,7} \end{bmatrix} = \begin{bmatrix} 1 & M_7 Y_7 \\ \dfrac{M_7}{Y_7} & 1 \end{bmatrix} \begin{bmatrix} p_7 \\ \\ \rho_o S_7 u_7 \end{bmatrix}, \tag{6}_1$$

which results in

$$\frac{v_{c,7} - M_7 p_{c,7}/Y_7}{1 - M_7^2} = \rho_o S_7 u_7. \tag{6}_2$$

Substituting Eq. (6) into Eq. (5), one has

$$c_o\rho_o S_5 u_5 + S_5 M_5 p_5 = c_o\rho_o S_7 u_7 \left[1 - \frac{(\gamma-1)}{c_o} Y_7 K_c S_7 M_7^2 \right] + \left(M_7 S_7 p_7 + c_o\rho_o u_6 S_6 \right). \tag{7}$$

With aeroacoustic perturbation, the momentum equation for steady flow is

$$(p_o + p_5) S_5 + (\rho + \rho_5) S_5 (V_5 + u_5)^2 + c_{11}[(p_o + p_7) S_7 + (\rho + \rho_7) S_7 (V_7 + u_7)^2] + c_{12}(p_o + p_6) S_6 = 0, \tag{8}_1$$

where

$$c_{11} = -1; \qquad c_{12} = -1. \tag{8}_2$$

As derived by MUNJAL [6], after substitution of thermodynamic properties and neglecting the second-order terms, this yields

$$S_5 p_5 + 2\rho_o S_5 V_5 u_5 + S_5 M_5^2 p_5 = -c_{11}\left(S_7 p_7 + 2\rho_o S_7 u_7 + S_7 M_7^2\left[p_7 - (\gamma-1)k_c M_7 Y_7 \frac{v_{c,7} - M_7 p_{c,7}/Y_7}{1-M_7^2}\right]\right) - c_{12} S_6 p_6. \tag{9}$$

By Substituting Eq. (6) into Eq. (9) and a rearrangement, we have

$$S_5\left(1+M_5^2\right)p_5 + 2\rho_o c_o S_5 M_5 u_5 + c_{11}\left(S_7 + S_7 M_7^2\right)p_7 = -c_{11}\left(\frac{2S_7}{c_o} - \frac{(\gamma-1)K_c M_7^3 Y_7 S_7^2}{c_o}\right)\rho_o c_o u_7 - c_{12} S_6 p_6. \tag{10}$$

As the flow passes through the sudden changed area, a part of the acoustic energy is dissipated in the form of heat loss. With the acoustic perturbation, this yields

$$(p_{o,5} + p_5) + \frac{1}{2}\rho_o (V_5 + u_5)^2 = (p_{o,7} + p_7) + \frac{1}{2}\rho_o (V_7 + u_7)^2 + \frac{1}{2} K_c \rho_o (V_7 + u_7)^2. \tag{11}$$

By substituting the thermodynamic properties and neglecting the second-order terms in Eq. (11), we have

$$p_5 + \rho_o V_5 u_5 = p_7 + \rho_o V_7 u_7 + K_c \rho_o V_7 u_7. \tag{12}$$

With the rigid wall at the boundary, one has

$$\frac{p_6}{\rho_o c_o u_6} = -j\cot(kL_4). \tag{13}$$

By taking Eq. (13) into Eqs. (7), (10), and (12), the transfer matrix between pt5 and pt7 is thus illustrated as

$$\begin{pmatrix} p_5 \\ \rho_o c_o u_5 \end{pmatrix} = \begin{bmatrix} TR4_{1,1} & TR4_{1,2} \\ TR4_{2,1} & TR4_{2,2} \end{bmatrix} \begin{pmatrix} p_7 \\ \rho_o c_o u_7 \end{pmatrix}. \tag{14}$$

As the theoretical derivation between point 5 and point 7, three kinds of a governing equation with the same assumption between point 2 and point 4 are deduced as follows.

First, the equation of mass continuity between point 2 and point 4 with mean flow is expressed in Eq. (15).

$$c_o \rho_o S_2 u_2 + S_2 M_2 p_2 = c_o \rho_o S_4 u_4 + c_o \rho_o S_6 u_3 + S_4 M_4\left(p_4 - \frac{p_o}{C_v}\frac{R K_e M_4 Y_4}{p_o}\frac{v_{c,4} - M_4 p_{c,4}/Y_4}{1-M_4^2}\right), \tag{15}_1$$

or

$$c_o\rho_o S_2u_2 + S_2M_2p_2 = c_o\rho_o S_4u_4 + c_o\rho_o S_3u_3 + S_4M_4\left(p_4 - \frac{p_o(\gamma-1)K_eM_4Y_4}{p_o}\frac{v_{c,4} - M_4p_{c,4}/Y_4}{1-M_4^2}\right), \quad (15)_2$$

where

$$K_e = \left[\frac{S_4}{S_2} - 1\right]^2. \quad (15)_3$$

A concept of static enthalpy deduced by MUNJAL [5, 6] is described as

$$\begin{bmatrix} p_{c,4} \\ v_{c,4} \end{bmatrix} = \begin{bmatrix} 1 & M_4Y_4 \\ \dfrac{M_4}{Y_4} & 1 \end{bmatrix} \begin{bmatrix} p_4 \\ \rho_o S_4u_4 \end{bmatrix}. \quad (16)$$

Substituting Eq. (16) into Eq. (15), one has

$$c_o\rho_o S_2u_2 + S_2M_2p_2 = c_o\rho_o S_4u_4\left[1 - \frac{(\gamma-1)}{c_o}Y_4K_cS_4M_4^2\right] + \left(M_4S_4p_4 + c_o\rho_o u_3S_3\right). \quad (17)$$

The equation of momentum for steady flow is

$$S_2p_2 + 2\rho_o S_2V_2u_2 + S_2M_2^2p_2 = -c_{21}\left(S_4p_4 + 2\rho_o S_4u_4 + S_4M_4^2\left[p_4 - (\gamma-1)k_eM_4Y_4\frac{v_{c,4} - M_4p_{c,4}/Y_4}{1-M_4^2}\right]\right) - c_{22}S_3p_3, \quad (18)_1$$

where

$$c_{21} = -1; \qquad c_{22} = 1. \quad (18)_2$$

Substituting Eq. (16) into Eq. (18), we have

$$S_2\left(1+M_2^2\right)p_2 + 2\rho_o c_o S_2M_2u_2 + c_{21}\left(S_4 + S_4M_4^2\right)p_4 = -c_{21}\left(\frac{2S_4}{c_o} - \frac{(\gamma-1)K_eM_4^3Y_4S_4^2}{c_o}\right)\rho_o c_o u_4 - c_{22}S_3p_3. \quad (19)$$

The equation of energy conservation for steady flow is

$$p_2 + \rho_o V_2u_2 = p_4 + \rho_o V_4u_4 + K_e\rho_o V_4u_4. \quad (20)$$

With the rigid wall at boundary, one has

$$\frac{p_3}{\rho_o c_o u_3} = -j\cot(kL_2). \tag{21}$$

By taking Eq. (21) into Eqs. (17), (19), and (20), the transfer matrix between pt2 and pt4 is thus illustrated as

$$\begin{pmatrix} p_2 \\ \rho_o c_o u_2 \end{pmatrix} = \begin{bmatrix} TR2_{1,1} & TR2_{1,2} \\ TR2_{2,1} & TR2_{2,2} \end{bmatrix} \begin{pmatrix} p_4 \\ \rho_o c_o u_4 \end{pmatrix}. \tag{22}$$

2.3. Combination of system matrix

Using the matrix substitution on Eqs. (1)–(3), (14), and (22), one has

$$\begin{pmatrix} p_1 \\ \rho_o c_o u_1 \end{pmatrix} = \begin{bmatrix} T11^* & T12^* \\ T21^* & T22^* \end{bmatrix} \begin{pmatrix} p_8 \\ \rho_o c_o u_8 \end{pmatrix}. \tag{23}$$

The sound transmission loss (STL) [6] of muffler is defined as

$$\begin{aligned} \text{STL}(Q, f, D_1, D_2, L_1, L_5, L_2, L_3) &= \text{STL}(Q, f, D_1, D_2, rt1, rt2) \\ &= 20\log\left(\frac{|T11^* + T12^* + T21^* + T22^*|}{2}\right) + 10\log\left(\frac{S_1}{S_8}\right), \end{aligned} \tag{24}_1$$

where

$$\begin{aligned} rt1(L_2) &= \frac{L_2}{L_3}; \\ rt2(L_4) &= \frac{L_4}{L_3}; \\ L_3 &= (L_o - L_1 - L_5)/(rt1 + rt2 + 1), \\ L_3 &= L_o - L_1 - L_2 - L_4 - L_5 = (L_o - L_1 - L_5)/(rt1 + rt2 + 1). \end{aligned} \tag{24}_2$$

3. Model check [8]

Before performing the GA optimal simulation on mufflers, the accuracy check of the mathematical model on the single-chamber muffler with extended tubes is made by experimental data [8]. As depicted in Fig. 3, the accuracy comparisons between the theoretical and experimental data for the models proved that they are in a good agreement. Therefore, the proposed fundamental mathematical model is surely valid under the cutoff frequency of $f = 3.83c/\pi D$ in which D is the diameter of the muffler.

In other words, when the target frequency is beyond the frequency range, the plane wave theory will not be applicable due to the high order mode wave being induced. Consequently, the models linked with the numerical method are applied for the shape optimization in the following section.

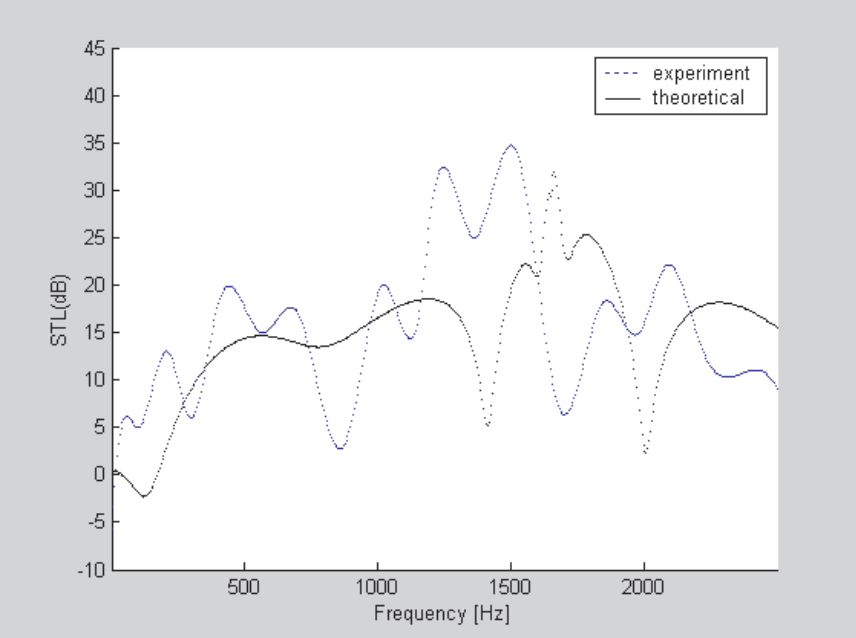

Fig. 3. Performance of a single-chamber muffler with extended tubes at the mean flow velocity of 3.4 (m/sec) [$D_1 = D_2 = 0.0365$ (m); $D_0 = 0.108$ (m); $L_1 = L_5 = 0.1$ (m); $L_2 = L_4 = 0.052$ (m); $L_3 = 0.104$ (m)].

4. Genetic algorithm

The Genetic Algorithm (GA) is a search algorithm based on the mechanisms of natural selection, one of the most important principles of Darwin: survival of the fittest. The technique uses a population of potential solutions represented by binary strings (called chromosomes or individuals) which is submitted to many transformations (called genetic operation such as selection, crossover, mutation and elitism). When either of a stationary state of the solutions candidate is reached or the specified accuracy criterion is met, the GA optimization is completed.

In the following we give a short description of the genetic algorithm which is applied as the optimizer in the shape optimization of the muffler hybridized with an extended tube.

A. Populations and Chromosomes

The initial population is built up by randomization. The parameter set is encoded to form a string which represents the chromosome. By evaluation of the object function, each chromosome is assigned with a fitness.

B. Parents

By using the probabilistic computation weighted by the relative fitness, pairs of chromosomes are selected as parents. The weighted roulette wheel selection is then applied. Each individual in the population is assigned a space on the roulette wheel which is proportional to the individual relative fitness. Individuals with the largest portion on the wheel have the greatest probability to be selected as parent generation for the next generation. A typical selection scheme, a weighted roulette wheel, is depicted in Fig. 4.

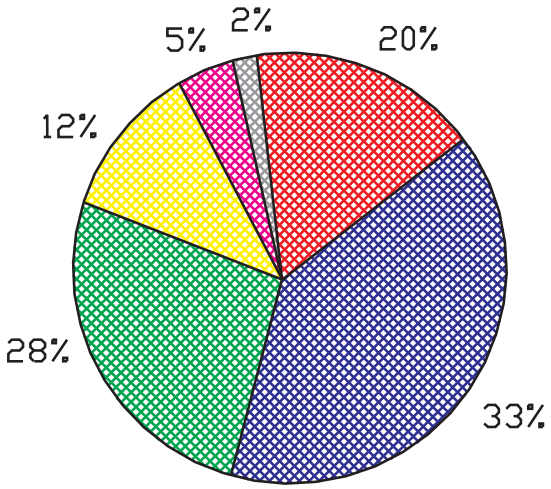

Fig. 4. Weighted roulette wheel method of selection.

C. Offspring

One pair of offspring is generated from the selected parent by crossover. Crossover occurs with a probability of *pc*. Both the random selection of a crossover and the combination of the two parent's genetic data are then preceded. The scheme of a single-point crossover is chosen in GA's optimization. Recombination and parent selection are the principle methods for the evolution in GA. A typical scheme of a single-point crossover is depicted in Fig. 5.

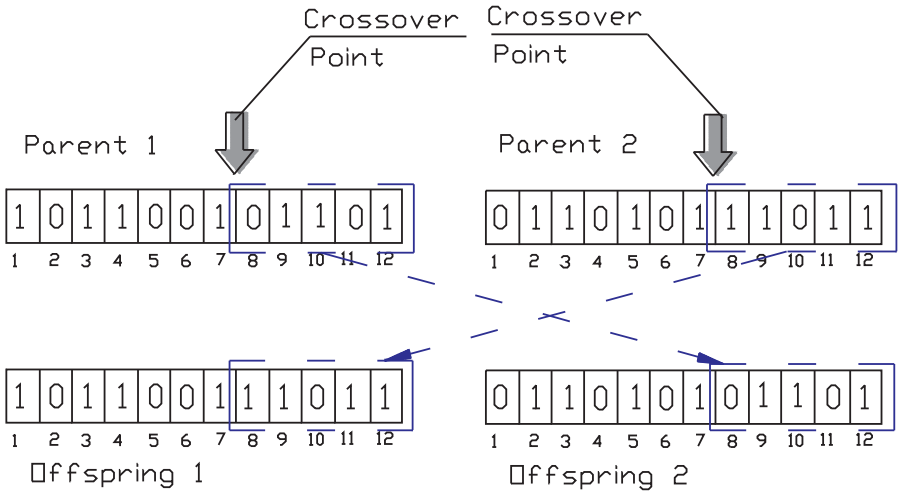

Fig. 5. Scheme of the single-point crossover.

D. Mutation

Genetically, mutation occurs with a probability of *pm* of which the new and unexpected point will be brought into the GA optimizer's search domain. It is an essential operation to improve the accuracy of GA's optimization. A typical scheme of mutation is depicted in Fig. 6.

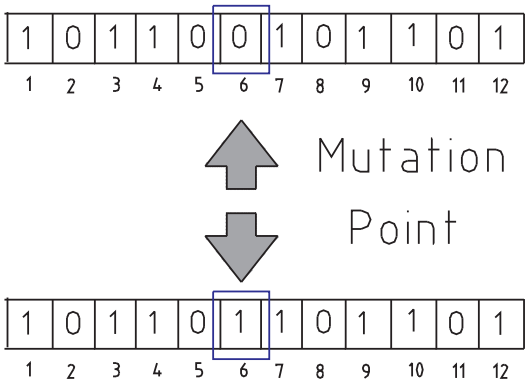

Fig. 6. Scheme of mutation.

E. Elitism

To prevent the best gene from the disappearance and improve the accuracy of optimization during reproduction, the elitism scheme to keep the best gene in the parent generations is thus presented and developed.

F. New Generation

Reproduction includes selection, crossover, mutation and elitism. The reduplication continues until a new generation is constructed and the original generation is substituted. Highly fit characteristics produce more copies of themselves in the subsequent generation resulting in a movement of the population towards an optimal direction. The process can be terminated when the number of generations exceeds a pre-selected value.

The operation in the GA method is shown in Fig. 7. The GA optimizer developed for a muffler hybridized with an extended tube is depicted in Fig. 8.

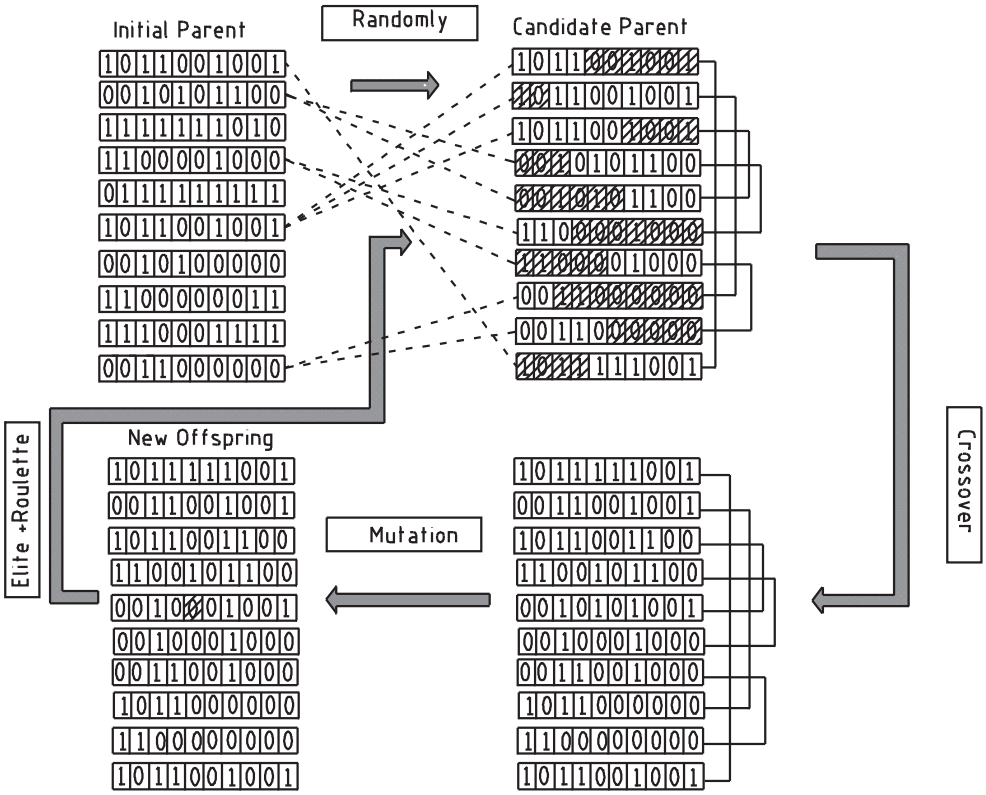

Fig. 7. Operation in the GA method.

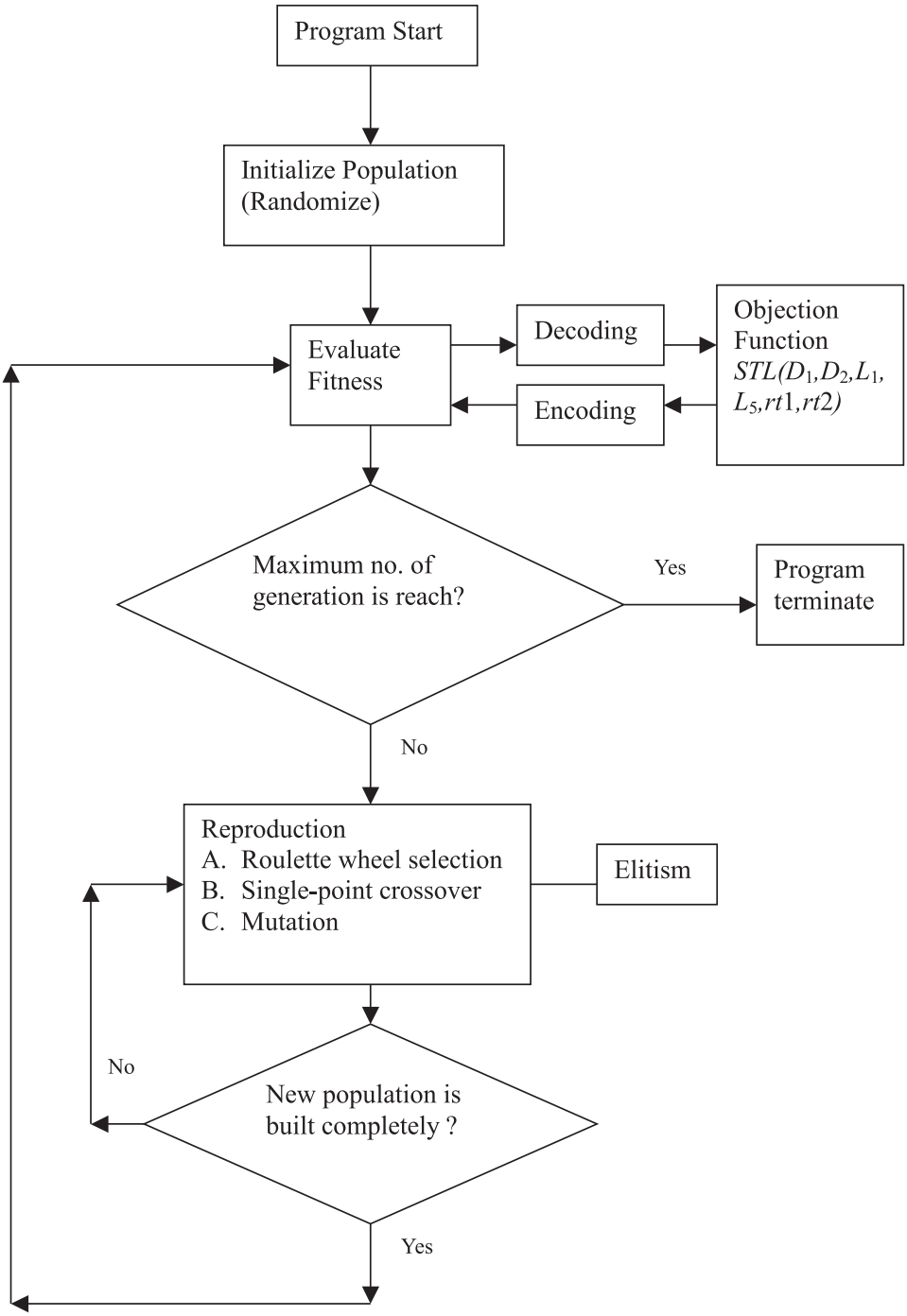

Fig. 8. Block diagram of GA optimization on the muffler.

5. Case study

A noise control of the gas venting device with pure tone noise at the exhausted outlet is introduced as the numerical case. With the narrow band's Fast Fourier Transform (FFT) analysis, a pure tone with higher noise level at 500 Hz is found. An intention of eliminating the pure tone noise is proposed in this study. A new muffler hybridized with extended tube is used. The available space for the muffler is 0.5 meter in width, 0.5 meter in height and 3.0 meter in length, respectively. In addition, GA is the chosen as optimizer to deal with the constrained problem in muffler's shape optimization. By Eq. (14), six design parameters are chosen in the GA optimization. To avoid a larger pressure drop and flow's generated noise occurring in the muffler [9], the minimal diameters at D_1 and D_2 are specified to be no less than 0.0762 (m) of which is the diameter of the venting device. In addition, for easily manufacturing the muffler, each segment of the muffler is limited so that to be not less than 0.1 (m). A series of assumptions of the constrained conditions in the design are illustrated as

$$0.0762(\mathrm{m}) \le D_1 \le 0.5\,(\mathrm{m}),\quad 0.0762(\mathrm{m}) \le D_2 \le 0.5\,(\mathrm{m}),\quad 0.1\,(\mathrm{m}) \le L_1 \le 0.5\,(\mathrm{m}),$$
$$0.1\,(\mathrm{m}) \le L_5 \le 0.5\,(\mathrm{m}),\quad 0.2 \le rt1 \le 2.0,\quad 0.2 \le rt2 \le 2.0,\quad f = 500\,(\mathrm{Hz})$$

The space constraint for muffler is shown in Fig. 9, and the design volume flow rate (Q) is confined to 0.8 (m^3/s).

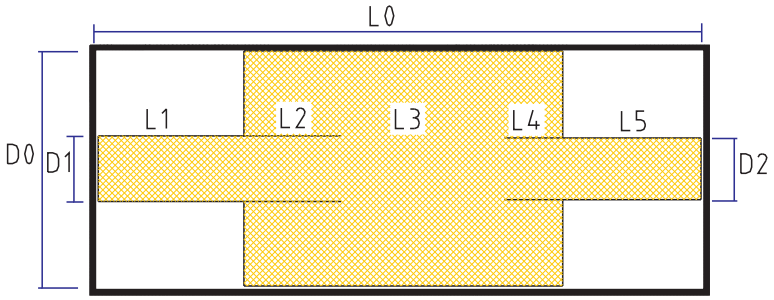

Fig. 9. Space constraints for a single-chamber muffler with extended tube [$L_0 = 3.0\,(\mathrm{m})$, $D_0 = 0.5\,(\mathrm{m})$].

6. Results and discussion

6.1. Results

The number of population (*popuSize*) is set as 60. The maximum generation (*gen_no*) is set as 500. The bit length is set as 40 (*bit_n*). According TO JOHNSON and YAHYA [10], both the typical ratio crossover (*pc*) and the mutation ratio (*pm*) used

in the following GA optimization are chosen as 0.8 and 0.05 individually. The optimization system is programed by MATLAB and run in IBM PC – Pentium IV. To achieve a better approach in GA, four trial cases with different values of those control parameters (*pc*, *pm* and *elt_no*) are thus to be varied and discussed. Respectively, other parameters such as *bit_n*, *popuSize*, *gen_no* are fixed to be of the same value. Four cases chosen are described as follows,

A. Case 1: pc=0.8, pm=0.05, elt_no=1

By using the crossover of 0.8 and mutation of 0.05, the GA optimization is preceded accompanied with the elitism of 1. The result shows that the best generation occurred at generation # 459. The best values of the design parameters – D_1, D_2, L_1, L_5, $rt1$, $rt2$ are found to be 0.0861 (m), 0.0861 (m), 0.1488 (m), 0.2602 and 1.8602, respectively. The optimal value of STL on the muffler is 176.7 (dB) with respect to those design parameters. In addition, the computation time of the optimization process is 2.30 minutes. The response of the GA optimization with respect to generations is shown in Fig. 10. As indicated in Fig. 10, the optimal process is obviously stable and more aggressive.

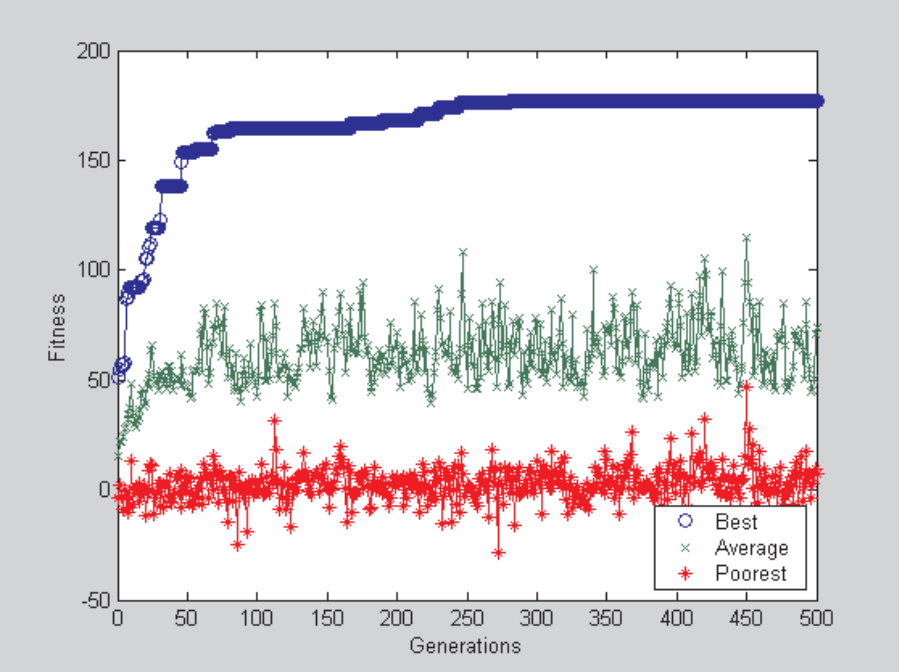

Fig. 10. GA optimization with respect to generations in case 1.

B. Case 2: pc=0.8, pm=0.05, elt_no=0

By using the crossover of 0.8 and the mutation of 0.05, the GA optimization is preceded accompanied with the elitism of 0. The result shows that the best generation occurred at generation # 210. The best values of the design parameters – D_1, D_2, L_1, L_5, $rt1$, $rt2$ are found to be 0.0861 (m), 0.0781 (m), 0.3117 (m), 0.1297 (m), 1.0634 and 1.0010, respectively. The optimal value of STL on the muffler is 152.2 (dB) with respect to those design parameters. In addition, the computation time of the optimization process is 2.44 minutes. The response of the GA optimization with respect to generations is shown in Fig. 11. As shown in Fig. 11, the fluctuation of best solution is violent. By no means, the GA optimal process becomes unstable with the lack of the elitism scheme.

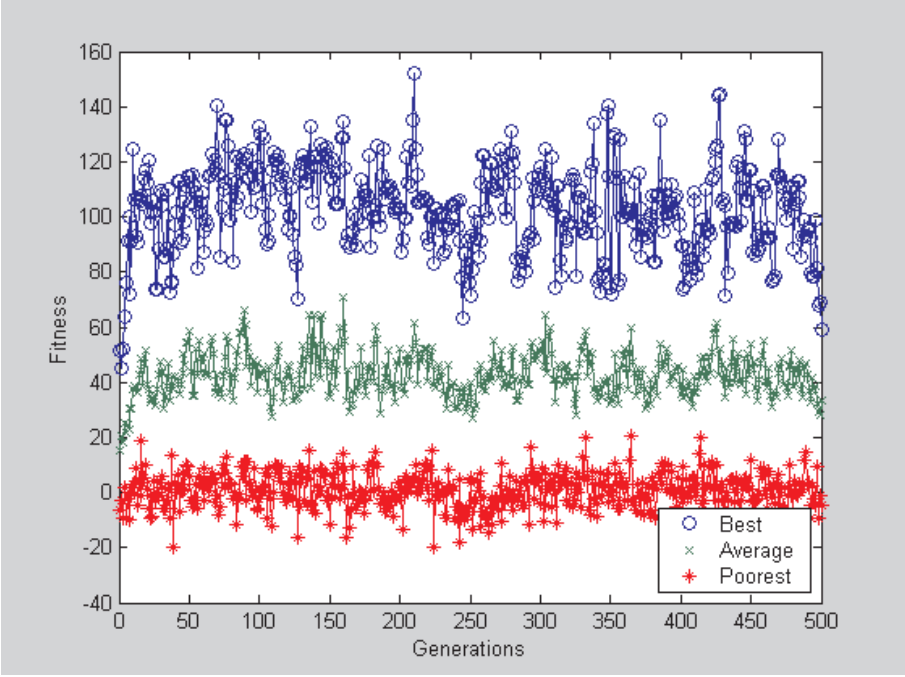

Fig. 11. GA optimization with respect to generations in case 2.

C. Case 3: pc=0.8, pm=0, elt_no=1

By using the crossover of 0.8 and the mutation of 0.0, the GA optimization is preceded accompanied with the elitism of 1. The result shows that the best generation occurred at generation # 25. The best values of the design parameters – D_1, D_2, L_1,

L_5, $rt1$, $rt2$ are found to be 0.0861 (m), 0.4909 (m), 0.4780 (m), 0.4303 (m), 1.5214 and 1.7902, respectively. The optimal value of STL on the muffler is 90.2 (dB) with respect to those design parameters. In addition, the computation time of the optimization process is 2.29 minutes. The response of the GA optimization with respect to generations is shown in Fig. 12. As illustrated in Fig. 12, the diversity of population is inefficient after a long term of generation. Therefore, a worse solution will be obtained with the lack of a mutation scheme.

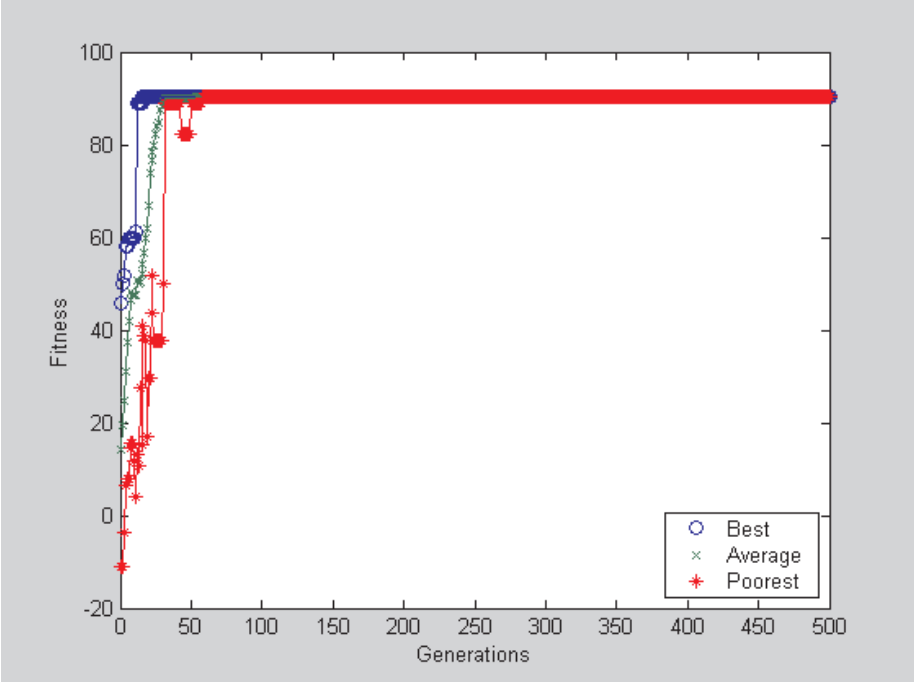

Fig. 12. GA optimization with respect to generations in case 3.

D. Case 4: pc=0, pm=0.05, elt_no=1

By using the crossover of 0.0 and the mutation of 0.05, the GA optimization is preceded accompanied with the elitism of 1. The result shows that the best generation occurred at generation # 359. The best values of the design parameters – D_1, D_2, L_1, L_5, $rt1$, $rt2$ are found to be 0.0858 (m), 0.0763 (m), 0.1423 (m), 0.3207 (m), 1.6996 and 0.7053, respectively. The optimal value of STL on the muffler is 96.3 (dB) with respect to those design parameters. In addition, the computation time of the optimization process is 2.18 minutes. The response of the GA optimization with respect to generations is shown in Fig. 13. As shown by the result in Fig. 13, the optimization is inert

with the lack of a crossover scheme.

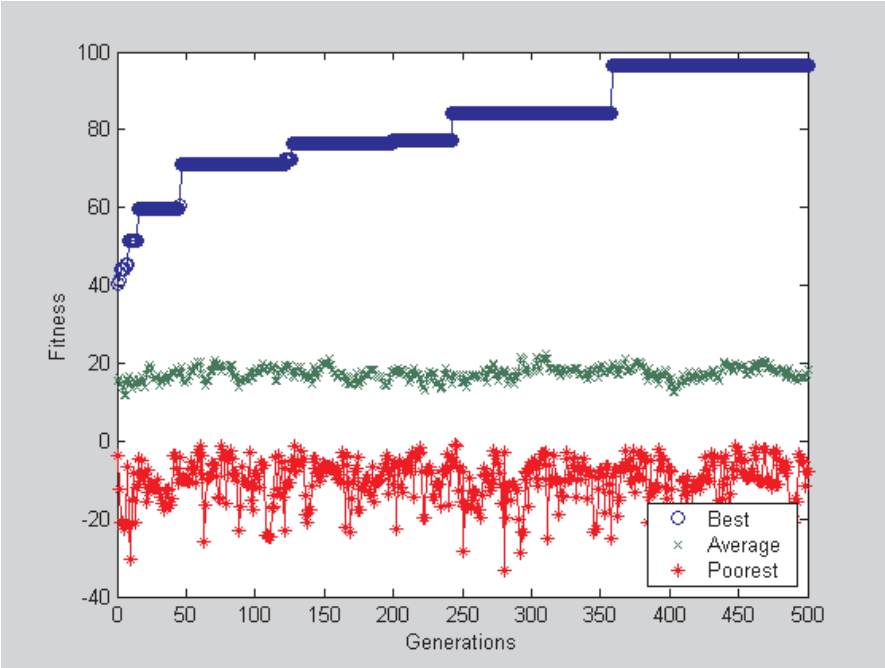

Fig. 13. GA optimization with respect to generations in case 4.

6.2. *Discussion*

The comparison of the optimizations in four cases is illustrated in Table 1. As indicated in Table 1, the 1-st case of which the crossover and the mutation/elitism were applied has the optimal value of STL compared with the other cases. The optimal STL

Table 1. Comparison of results for variations of the control parameters.

	Common parameters			Control parameters			Results							Elapsed time
	PopuSize	*gen_no*	*bit_no*	*pc*	*pm*	*elt_no*	D_1(m)	D_2(m)	L_1(m)	L_5(m)	*rt*1	*rt*2	STL	t (min.)
Case1	60	500	40	0.8	0.05	1	0.0861	0.0861	0.1488	0.2602	0.2566	1.8602	176.7	2.30
Case2	60	500	40	0.8	0.05	0	0.0861	0.0781	0.3117	0.1297	1.0634	1.001	152.2	2.44
Case3	60	500	40	0.8	0	1	0.0861	0.4909	0.4780	0.4303	1.5214	1.7902	90.2	2.29
Case4	60	500	40	0	0.05	1	0.0858	0.0763	0.1423	0.3207	1.6996	0.7053	94.9	2.18

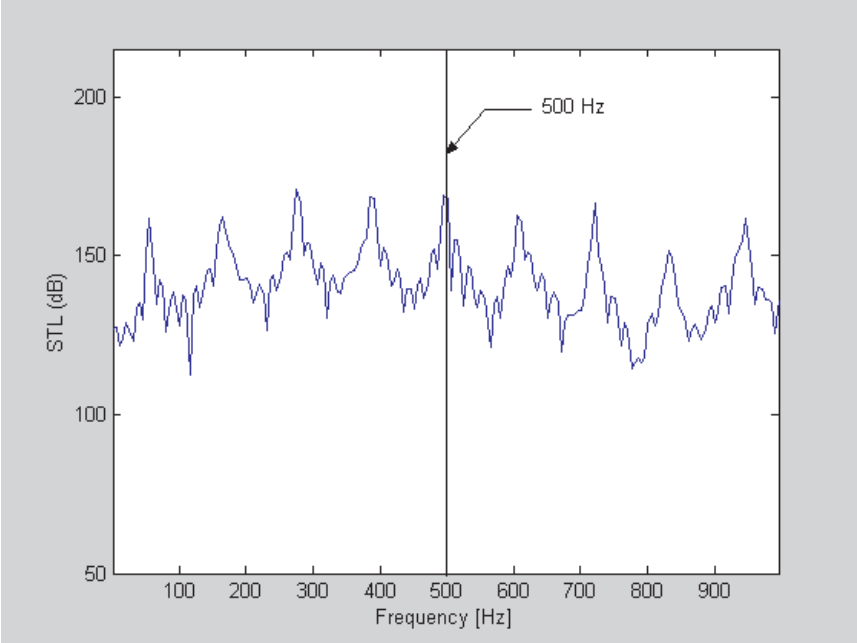

Fig. 14. Optimal STL with respect to frequency.

with respect to the spectrum is shown in Fig. 14. It indicates that the maximum value of STL is obtained at the peak of the profile of which the corresponding frequency is coincidence with the desired frequency of 500 Hz. Therefore, the optimal design of the muffler is acceptable.

7. Conclusion

It has been shown that GA can be used in the optimization of a muffler system under the space constraints. Because of no starting design, GA becomes easier to be used. The case study reveals that the GA parameters play an essential role in the accuracy. Both the crossover/mutation and elitism are necessary in the GA optimization. Definitely, the result shows that optimal STL was maximized at the target frequency of 500 Hz. This proves that the GA optimization in a single expansion muffler with extended tube is applicable.

Acknowledgments

The authors would like to thank the reviewers for the helpful advices in the text.

References

[1] KAISER L., BERNHARDT H., *Noise control on computer and business equipment using speed control blowers*, IEEE, **2**, 114–117 (1989).

[2] BERNHARD R.J., *Shape optimization of reactive mufflers*, Noise Control Engineering Journal, **27**, 1, 10–17 (1986).

[3] YEH L. J., CHIU M. C., LAY G. J., *Computer aided design on single expansion muffler under space constraints*, Proceedings of the 19-th National Conference on Mechanical Engineering (The Chinese Society of Mechanical Engineers), C7, 625–633, Hu-wei, Taiwan 2002.

[4] MAN, TANG KWONG, *Genetic algorithms*, Springer, 1999.

[5] PRASAD M. G., *A note on acoustic plane waves in a uniform pipe with mean flow*, Journal of Sound and Vibration, **95**, 2, 284–290 (1984).

[6] MUNJAL M. L., *Acoustics of ducts and mufflers with application to exhaust and ventilation system design*, John Wiley & Sons, New York 1987.

[7] SATHYANARAYANA Y., MUNJAL M. L., *A hybrid approach for aeroacoustic analysis of the engine exhaust system*, Applied Acoustics, **60**, 425–450 (2000).

[8] WANG C. N., HSIEH C. C., *Experimental study for muffler components with flow*, Bulletin of the College of Engineering, N.T.U., **78**, 67–74 (2000).

[9] BIES D. A., HANSEN C. H., *Engineering noise control*, Unwin Hyman, UK, 1988.

[10] JOHNSON J. M., YAHYA R. S., *Genetic algorithm optimization and its application to antenna design*, Proceedings of the IEEE Antennas and Propagation Society International Symposium, 326–329, 1994.